LONG-DURATION EXPERIMENTS IN IRREGULAR WAVES, TO DETERMINE 10,000-YEAR WAVE LOADS ON A 3.5M DIAMETER VERTICAL CYLINDER

J.R.Chaplin, Civil, Maritime & Environmental Engineering & Science, University of Southampton, Southampton SO17 1BJ, UK *j.r.chaplin@soton.ac.uk*

R.C.T.Rainey*, Oil & Gas Division, Atkins Ltd., Euston Tower, 286 Euston Road, London NW1 3AT, UK *rod.rainey@atkinsglobal.com*

Introduction

Extreme wave loads are of great practical importance in the offshore oil industry – increasingly so, as rising safety standards have demanded the consideration of 10,000-year extreme cases as well as the traditional 100-year extremes. A single vertical cylinder is the simplest case, and one of 3.5m diameter is relevant to more modern designs of oil rig, with fewer structural members, but of a larger diameter.

At this diameter the wave load is normally dominated by the inertia term in Morison's equation (see e.g. [1], p.224), but in extreme conditions (wave height > $2\pi \times$ diameter = 22m) the drag term dominates. The design codes (e.g. [2] Sec.3.3.3) recommend that the wave load be calculated using Morison's equation, with velocity and acceleration defined by "Grue's method" [3], i.e. fitting regular wave models to the elevations of individual waves.

The present experiments explore whether this approach is adequate for determining 10,000-year wave loads, which must include a consideration of the variability of the 100-year extreme load, since there are 100 of them in 10,000 years.

Experimental set-up

The measurements were carried out in the narrow wave flume at Southampton University, 18m long, 0.42m wide, with a still water depth of 0.7m. The flume is equipped with a bottom-hinged wave paddle with active absorption at one end, and a large volume of firm polyether foam at the other. As in other recent investigations of extreme wave events [4], no 2nd order correction was applied to the wave paddle motion. Measurements in regular waves indicated that reflections from the polyether foam beach were about 4.5%, 2.8% and 2.8% at 0.75Hz, 1.0Hz and 1.5Hz respectively.

Wave loading tests were carried out in 10 different storm conditions, with a single vertical cylinder mounted on the centreline of the tank at 6.5m from the paddle. In fact three test cylinders were used in turn, with diameters corresponding to a 3.5m leg at 3 different scales. The scales were chosen so as to keep the wave frequencies in each storm comfortably within the operating range of the wave paddle. Details are given in Table 1. Waves were generated with JONSWAP target spectra, comprising 200 frequency components at unequal intervals, with peak enhancement factor 3.3.

The cylinders were 860mm long carbon fibre tubes. They were flooded internally during the tests, but were largely filled with foam to prevent internal sloshing. They were mounted on load cells at top and bottom with connections that were virtually moment-free. When installed, the fundamental natural frequency of each cylinder was close to 21Hz. A wave gauge was placed alongside the cylinder. The tests ran continuously for the equivalent of 72.5 full scale hours, providing 24 realisations of the 3-hour storm. All channels were filtered at 100Hz and sampled at 200Hz.

Wave breaking

Particularly in the sea-states with steepest waves, breaking could be observed at frequent intervals over the whole length of the tank, and images of the wave motion at the cylinder confirmed that the highest force peaks were associated with impacts in breaking waves. In an attempt to identify these events throughout each test, we computed the curvature of the force record at each force peak. Cases of wave impact had sharp peaks and often discontinuities in the rate of change of force. Plots of the probability distribution of force peak curvatures reveal a change of slope that is not present in time-stepping simulations, see Fig. 1. When the curvature exceeds that at which this change occurs C_{crit} we have assumed that the force peak is significantly influenced by a wave breaking on the cylinder.

---

* Presenting author

Storm	Full scale		Scale	Model scale			
	H_s (m)	T_p (s)		diam. (mm)	H_s (mm)	T_p (s)	S
1	9.7	10	140	25.0	68.3	0.845	0.061
2	10.9	11	140	25.0	75.5	0.930	0.056
3	11.8	12	140	25.0	85.9	1.014	0.054
4	13	13.3	168	20.8	75.3	1.026	0.046
5	13.5	14	168	20.8	80.4	1.080	0.044
6	14	14.9	210	16.7	66.1	1.028	0.040
7	14.2	15.9	210	16.7	68.0	1.097	0.036
8	14	16.8	210	16.7	66.0	1.159	0.031
9	13	17.6	210	16.7	63.7	1.215	0.028
10	11.4	18	210	16.7	54.5	1.242	0.023

Table 1. Test conditions based on a full scale leg diameter of 3.5m. The steepness $S = 2\pi H_s / g T_p^2$.

Using this curvature threshold it was possible to separate those force peaks that were, and were not, probably much affected by wave breaking. In Fig. 2 these populations are plotted separately for two sea-states. It can be seen that wave breaking can be associated with force peaks over almost the entire range. But by a considerable margin (a factor of up to 2 in storm 6), the highest force peaks occur in breaking waves.

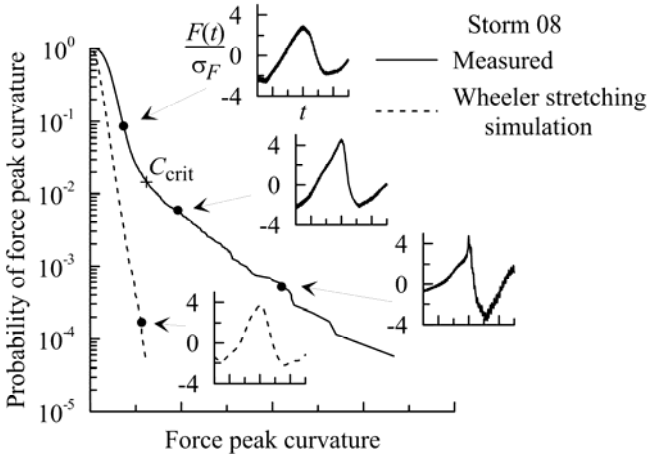

Figure 1. Probability distributions of the magnitude of the curvature d^2F/dt^2 at force peaks. The change in slope in the measured data at a curvature C_{crit} is taken as an indication of the onset of wave breaking on the cylinder.

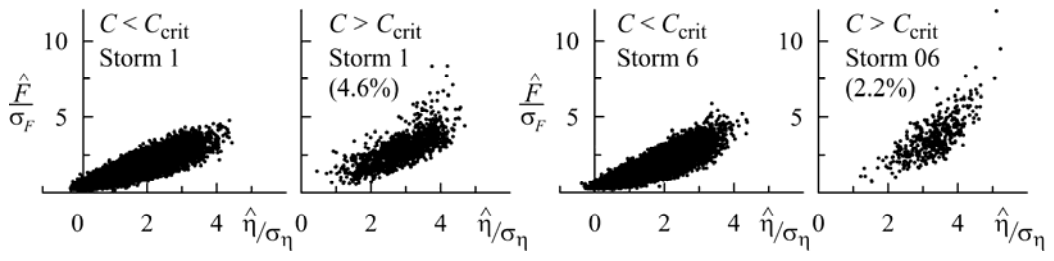

Figure 2. Individual force peaks plotted against the corresponding crest elevations. Data on both axes are normalised with respect to the standard deviation of the respective time series. Plots on the left and right are from nominally non-breaking and breaking waves respectively. Percentages represent the occurrence of the latter.

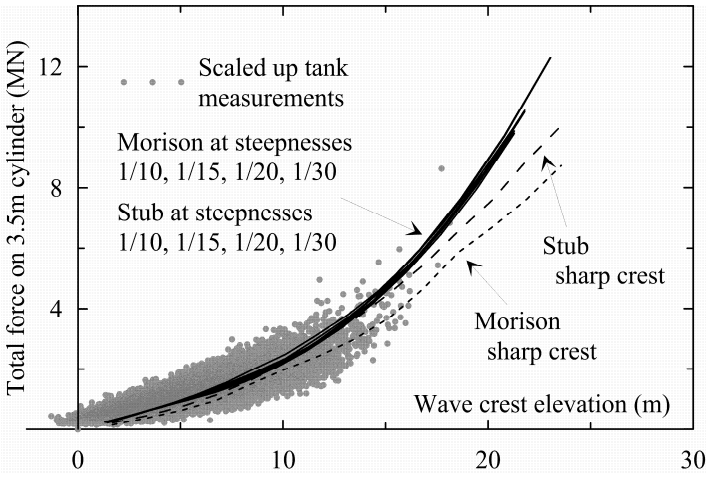

Figure 3. Scaled up tank measurements of peak forces and corresponding wave crest elevations from Storm 6 compared with predictions.

Wave Loads

The peak loads in successive waves are conveniently plotted against crest elevation in Fig. 3. On this plot, the predictions of "Grue's method" conveniently almost collapse to a single line, because the wave load up to the still water line from Morison's equation (both drag and inertia terms) is independent of wave period, since the increased velocity and acceleration with reduced period is exactly offset by the increased exponential decay-rate with depth. Results are shown for Stokes 2nd order waves, of various steeepnesses, with Morison drag and inertia coefficients of 2.0 and 1.2, which are appropriate to the Reynolds number of the experiments. Also shown are the results ("Stub") with the slender-body corrections [6], [7] to the Morison inertia term included – they are evidently negligible in these waves. Finally results are given for waves [8] with a 120-degree Stokes crest – the loads are less, presumably because the sharp crest increases the crest elevation more than the wave load. The results also vary noticeably with the inclusion of the slender-body corrections to Morison's equation – which are more noticeable in the sharp crest.

Although "Grue's method" predicts the correct loads on average, the striking feature of the results is the large scatter. This has been noted before, in full scale measurements [9], where "some waves appear to be more forceful than others", and it is of great practical importance because it is relevant to the 10,000-year extreme wave load, which must be at least as big as the wave load expected in 100 realisations of the 100-year storm. This is most easily seen by dividing the 72-hour time history into twenty-four 3-hour runs, and considering the maximum wave force seen in each. The average value of this maximum force over the twenty-four 3-hour runs, and its variability ±2σ ("95% confidence limits") is shown in Fig. 4. The upper 95% confidence limit is an indication of the 10,000-year extreme load – an under-estimate in fact, because assuming a Normal distribution, it has a 2.28% chance of being exceeded, and so will be exceeded in about fifty 100-year storms.

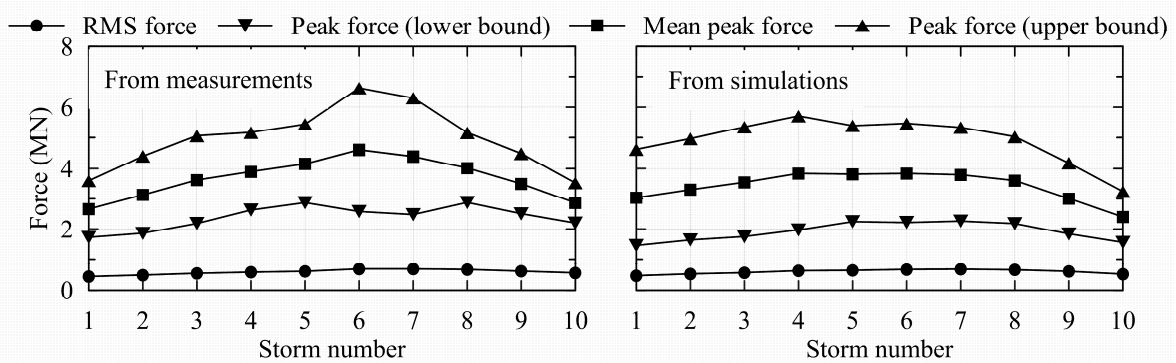

Figure 4. Average, and upper and lower bounds of maximum peak forces from the equivalent of twenty-four 3-hour runs at full scale. On the left are shown forces scaled up from the measurements, and on the right those obtained from simulations. Also shown is the RMS force for each storm.

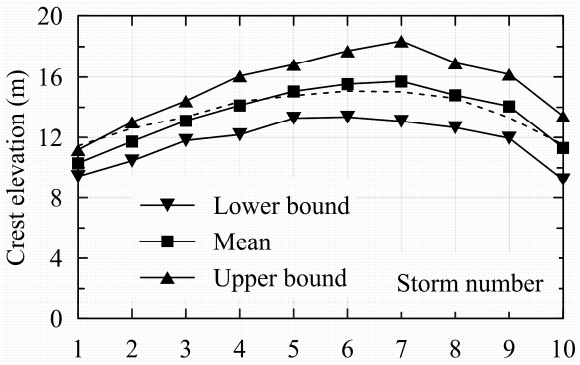

Figure 5. Scaled up average, and upper and lower bounds of measured maximum crest elevations from the equivalent of twenty-four 3-hour test runs at full scale. Expected maximum crest elevations based on Forristall's crest distribution [2,11] are shown as a broken line..

By contrast, the variability in wave crest elevation is much less (Fig. 5). If we predict wave loads by "Grue's method" then we will see the same small variability in wave load – or at most twice the variability, because of the contribution of the square-law Morison drag term. We will thus seriously underestimate the 10,000-year wave load. The explanation for the large variability in wave load remains elusive. It is argued in [5] that linear wave theory (without any "Wheeler stretching" [10]) remains valid in irregular waves, provided the wave spectrum is truncated to a 2:1 frequency range. The wave load calculated on this basis (and taking the 1st order surface elevation) is shown in Fig 2, and reproduces the observed scatter in wave load to a remarkable degree.

The implication is that linear wave theory, without any "stretching", remains a good model of wave kinematics in wave crests, provided the wave spectrum is truncated to a 2:1 frequency range. As highlighted in [5], this approximation also gives an explanation of wave breaking as "particle escape".

Conclusions

Very long-duration model experiments reveal great variability in the 3-hour extreme wave load on a 3.5m diameter vertical cylinder, with important implications for the 10,000-year wave load on offshore structures. The variability in 3-hour extreme load is much larger than the variability in 3-hour extreme crest elevation. Part of the explanation is wave breaking, but the results are most easily explained by assuming linear irregular-wave theory applies in the wave crests, without any "Wheeler stretching" and with only a truncation of the spectral width (to 2:1 frequency range). Such a view of irregular-wave kinematics also explains wave breaking as "particle escape".

The authors thank Talisman Energy Norge AS for financial support and permission to publish results.

References

[1] Faltinsen, O.M. 1990 *Sea Loads on Ships and Offshore Structures* CUP
[2] DNV-RP-C205 *Environmental Conditions and Environmental Loads*
[3] Grue, J. et al 2003 Kinematics of extreme waves in deep water. AOR 25, 355-366.
[4] Onorato, M. *et al.* 2009 Statistical properties of mechanically generated surface gravity waves: a laboratory experiment in a three-dimensional wave basin. JFM 627, 235-257.
[5] Rainey, R.C.T. 2007 Weak or strong nonlinearity: the vital issue, J. Eng Maths, 58 229-249
[6] Rainey, R.C.T. 1989 A new equation for calculating wave loads on offshore structures, JFM, 204, 295-324
[7] Rainey, R.C.T. 1995 Slender-body expressions for the wave load on offshore structures. Proc.R.Soc. A450 391-416
[8] Longuet-Higgins, M.S. 1973 On the form of the highest progressive and standing waves in deep water. Proc.R.Soc. A331 445-456
[9] Heideman, J. C. & Weaver, T. O. 1992. Static wave loading procedure for platform design. Proc. ASCE, Civ. Engrg. in the Oceans V, 496–519
[10] Wheeler, J.D.E. 1970 Method for calculating forces produced by irregular waves. Journal of Petroleum Tech.,249 359-367.
[11] Forristall, G.Z. 2000 Wave crest distributions: observations and second-order theory. J. Phys. Ocean. 30, 1931-1943.